International Journal of Heat and Fluid Flow 73 (2018) 188–198

Contents lists available at ScienceDirect

International Journal of Heat and Fluid Flow

journal homepage: www.elsevier.com/locate/ijhff

Unsteady pressure analysis of the near wall flow downstream of the front wheel of a passenger car under yaw conditions

Sabine Bonitz[*,a], Lars Larsson[b], Simone Sebben[c]

[a] Vehicle Engineering & Autonomous Systems, Department of Mechanics and Maritime Sciences, Chalmers University of Technology, Gothenburg, Sweden
[b] Marine Technology, Department of Mechanics and Maritime Sciences, Chalmers University of Technology, Gothenburg, Sweden
[c] Vehicle Engineering & Autonomous Systems, Department of Mechanics and Maritime Sciences, Chalmers University of Technology, Gothenburg, Sweden

ABSTRACT

The flow around passenger cars is complex and is characterized by many different structures and interactions. The occurring flow phenomena around a car determine crucial vehicle properties such as the driving stability, the noise level, the aerodynamic performance and the vehicle contamination. Therefore, it is of high importance to increase the understanding of the developing flow phenomena. Generic models are widely used to investigate flow structures and their interactions, but cannot serve to derive a general flow field for detailed full-scale vehicle models. A particularly complex area is the flow around the wheels and its interaction with the vehicle geometry. Studies on wheel-wheelhouse flow focus mainly on the geometrical influence of the wheel size, rim and tyre on the aerodynamic drag and the flow field close to the wheel. The present work investigates the flow behind the front wheel arch of a full-scale passenger car. Time resolved surface pressure measurements were taken to study the near wall flow under different yaw conditions. Based on the data obtained, flow structures are identified and their propagation speed is calculated. Further, characteristic frequencies observed are discussed. It is found that coherent structures are present behind the front wheel arch, one above the wheel centre height and one below it. These remain even under large yaw angles, no matter if the vehicle is yawed to lee- or windward. The investigation further shows that two characteristic frequencies can be found, $St = 0.03$ and $St = 0.2$, whereby the latter is caused by the wheel rotation. The same frequencies also occur under yaw conditions, but yawing the measurement area to leeward results in less pronounced frequency peaks.

1. Introduction

The flow around passenger cars is a highly complex, three dimensional bluff body flow, which is characterized by vortices and recirculation regions of different sizes. The created flow structures interact with each other and determine crucial vehicle properties such as the driving stability, the noise level in the passenger compartment and the aerodynamic performance. Equally, it is important to understand the flow field when vehicle soiling is considered. Apart from the customers demands not to touch dirty handles or to soil their clothes, safety aspects such as driver visibility have to be considered. The usage of sensors and radars is increasing, especially with the development of autonomous systems. To ensure their functionality, it is crucial to avoid their contamination.

To be able to understand the complex flow field around vehicles, generic bodies such as the Ahmed body or the SAE model are often used to study the development and impact of the resulting flow structures; for instance in Gulyás et al. (2013); Bruneau et al. (2014); Rossitto et al. (2016); Meile et al. (2016). The study of simplified models allows the identification of main features and to look into the impact of different effects, such as the influence of edge radii. In the development of full vehicle geometries, findings regarding geometrical improvements from the generic studies are combined and the different resulting flow phenomena interact with each other in a new context. Hence, it is also necessary to study detailed vehicle models. These further allow one to consider flow situations of the full vehicle, such as the flow through the engine bay and around the wheels (Landström, 2011; Hobeika et al., 2017).

The flow around the wheels and through the wheelhouses receives high attention. This is mainly due to its complexity. First, the wheel is rotating in contact with the ground. Therefore, the simulation of the driving condition has to be considered. Second, the wheel-vehicle interaction creates complex flow structures that are highly unsteady and sensitive to different parameters, for instance the rim design, tyre pattern or wheel size (Wäschle, 2007; Zhiling et al., 2010; Landstrom et al., 2012; Landström et al., 2011b; 2011a; Hobeika et al., 2013; Schnepf et al., 2015).

Simulating the driving conditions requires wheel rotation and a moving ground representation. Automotive wind tunnels are therefore equipped with moving belt systems, which rotate the wheels and simulate the moving road. It is not enough to understand the flow around an isolated wheel, but also around rotating wheels, and its interaction with the remainder of the vehicle. The wheel-vehicle interaction complicates the study, as flow phenomena cannot be isolated and studied individually.

* Corresponding author.
E-mail addresses: sabine.bonitz@chalmers.se (S. Bonitz), lars.larsson@chalmers.se (L. Larsson), simone.sebben@chalmers.se (S. Sebben).

https://doi.org/10.1016/j.ijheatfluidflow.2018.07.007
Received 2 January 2018; Received in revised form 18 July 2018; Accepted 18 July 2018

Isolated wheel investigations were done for instance by Axon et al. (1998); Wäschle (2007); Schnepf et al. (2015); Dimitriou and Klussmann (2006); Emma Croner et al. (2013). The flow topology of an isolated rotating wheel is for instance shown by Wäschle (2007). As a main structure, a horseshoe vortex behind the wheel is reported. This vortex is responsible for the main drag of the wheel and becomes weaker with wheel rotation. On the upper side of the wheel, a separation is created that has a ring vortex shape and causes an increase in pressure on top and behind the wheel, which reduces drag. The third observed structure is a vortex around the wheel shoulder at ground contact, which is weaker compared to the horseshoe vortex. Schnepf et al. (2015) explained, on an isolated wheel, the sensitive connection between tyre pattern and tyre load. Their results give insight into the significant changes of the wheel wake due to changes in these parameters.

Taking the wheel - wheelhouse and under body interaction into account, changes the topology around the wheel and its flow structure interactions (Dimitriou and Klussmann, 2006; Landström et al., 2009; Wäschle, 2007; Tamas Regert and Tamas Lajos, 2007; Söderblom, 2012). Wäschle (2007) showed the topology for a wheel-wheelhouse configuration. Due to the wheelhouse, the upper ring vortex described for the isolated wheel is no longer present. The horseshoe vortex created in the wheel wake and the vortices created at the lower shoulders still existent though. At the rim flange, a rim vortex appears. For a stationary configuration it has the shape of a horseshoe. Due to the wheel rotation, the upper part of this horseshoe vortex is almost nonexistent. It is explained that for a stationary wheel the upper vortex trail is fed by the flow exiting the gap between wheel and wheelhouse. For a rotating wheel, the mass flow exiting this gap is lower and therefore the upper vortex trail is not preserved. The lower vortex trail is fed by the flow through the rim and therefore dependent on the rim design. The only vortex that occurs in the study purely due to wheel rotation is a longitudinal one appearing at the side, approximately at the wheel centre height. It is explained that this vortex is created due to the movement of the wheel wall against the flow direction. The rotation causes reverse flow on the upper wheel part and a separation bubble at the front side of the tyre. Due to the reverse flow, a rotation is induced that causes the side vortex.

The flow physics downstream of the wheel arch are rarely investigated, especially its surface topology and surface pressure properties. In a numerical steady state investigation, done by Bonitz et al. (2015), the flow downstream of the front wheel and its development into the bulk flow is discussed based on surface streamlines (limiting streamlines) and 2D streamlines in cross planes, as well its surface pressure. It was discussed, how the limiting streamlines correlate with flow structures observable in the flow and how the surface properties can give insight into the occurring flow phenomena. In a further investigation (Bonitz et al., 2018), limiting streamlines obtained from experiments on a full scale vehicle were correlated with time resolved pressure measurements. Fluctuations of the tuft movement and the pressure were studied and coherent structures in the flow were identified.

Apart from the aerodynamic impact, the created flow determines the level of contamination. Particles risen by the wheel rotation are transported downstream, stick to the vehicle's side and accumulate. Gaylard and Duncan (2011) as well as Gaylard et al. (2017) describe in their work the significant level of contamination onto the side of a SUV and a notchback car due to the wheel wake flow. Experimental and numerical investigations have shown that the side soiling is mainly caused by flow being driven out the wheel house. Therefore the importance of an improved front wheel house design is emphasized.

However, in order to reduce side contamination, a better understanding of the flow physics in this area is needed in order to estimate the wheel wake dimension and to understand its behavior due to structures created by the wheel-wheel house interaction under different conditions.

This work focuses on the near wall flow downstream of the front wheel of a fully detailed passenger car under different yaw conditions. Unsteady surface pressure measurements are used in order to study how different flow phenomena can be identified and how flow structures propagate downstream. The zero yaw case serves as the baseline configuration and its analysis is complemented by results obtained from CFD simulations. The wheel-wheelhouse flow is then altered by yawing the car to lee- and windward, which shows how the flow structure dimensions and their propagation is changed. For all flow configurations, the surface pressure, the RMS of the fluctuating pressure and the dominant frequencies are analysed. The study found coherent structures propagating downstream that remain even under large yaw angles. The spectral analysis showed that dominant frequencies can be found at $St = 0.2$ and $St = 0.03$, whereby $St = 0.2$ can be attributed to the wheel rotation. These frequencies are also present under yaw conditions, but appear to be less pronounced if the measurement location is yawed to leeward.

2. Experimental setup

Unsteady surface pressure measurements were taken downstream of the front wheel of a full-scale passenger car. The experiments were performed in the Volvo Cars aerodynamic wind tunnel in Gothenburg, Sweden. Fig. 1 shows the vehicle in the wind tunnel environment.

2.1. Wind tunnel

The wind tunnel is a closed loop building type with slotted walls in the test section (30% open area). The test section is 6.6 m wide, 15.8 m long and 4.1 m high, which leads to a cross sectional area of 27.06 m^2. The test object is fixed in its place by four rigid struts. To simulate the moving road, a boundary layer control systems and a five belt system are installed (see Fig. 1). The wheels are rotated by spinning the belts underneath each wheel (called wheel drive units). The installed turntable allows yawing of the vehicle up to $\pm$ 30°. During the experiment configurations at $\beta = 0°$, $\beta = \pm5°$, $\beta = \pm10°$ and $\beta = \pm15°$ were tested. Fig. 2 shows a schematic of the wind tunnel setup and its coordinate systems.

The flow is driven by a 5 MW fan and allows test speeds up to 250 km/h. The test speed in the experiment was 100 km/h, which corresponds to a Reynolds number of $Re = 6.1 \cdot 10^6$ based on the vehicle length (l= 4.63 m). The wind tunnel nozzle contraction ratio is 6:1 and the turbulence level at the center of the turntable is 0.1%. The blockage due to the car frontal area is 8% at zero yaw. A more detailed description about the wind tunnel and its road simulation can be found in Sternéus et al. (2007).

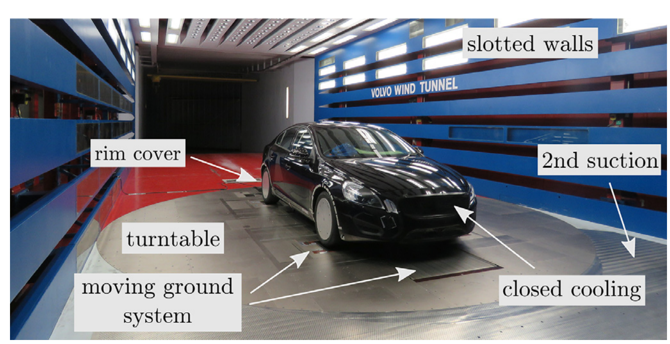

Fig. 1. Vehicle setup in the wind tunnel. (For interpretation of the references to colour in this figure legend, the reader is referred to the web version of this article.)